Dye-Sensitized Solid-State Photovoltaic Cells Based on Dye Multilayer−Semiconductor Nanostructures

V. P. S. Perera, P. K. D. D. P. Pitigala, P. V. V. Jayaweera, K. M. P. Bandaranayake, and K. Tennakone*

Institute of Fundamental Studies, Hantana Road, Kandy, Sri Lanka

Received: April 5, 2003; In Final Form: October 29, 2003

The efficiency of dye-sensitized solar cells may be further improved if ways are found to broaden the spectral response resolving the fundamental issues involved. Here we report construction of dye-sensitized solid-state photovoltaic cells with heterostructure configurations: [1] n-TiO_2/D_1/p-CuSCN, [2] n-TiO_2/*p-CuSCN*/D_2/p-CuSCN and [3] n-TiO_2/D_1/*p-CuSCN*/D_2/p-CuSCN, where n-TiO_2 is a ∼10 μm thick nanocrystalline film of titanium dioxide, *p-CuSCN* and p-CuSCN are thin (∼ 2 nm) and thick (∼ 10 μm) films of copper(I) thiocyanate. Monolayers of the dyes D_1 (Fast Green) and D_2 (Acridine Yellow) are coated on TiO_2 and *p-CuSCN*, respectively. The cell of configuration [3] delivered the highest efficiency, open-circuit voltage, and short-circuit photocurrent as it effectively utilizes the light adsorbed by D_1 and D_2. The mechanism of operation involves tunneling of energetic electrons and holes liberated in photoexcitations of dyes through a thin barrier of *p-CuSCN*. The strategy adopted indicates the possibility of designing more efficient dye-sensitized solar cells, widening the spectral response.

Photoexcited dye molecules anchored to a semiconductor surface could inject electrons to the conduction band (CB) or holes to the valence band (VB).[1,2] This process, known as dye-sensitization, affords a neat way of transferring energetic carriers of one type (either n or p) to a semiconductor. The electronic coupling of the dye molecule to the semiconductor surface causes fast electron injection,[3] effectively circumventing the dissipative processes that generally occur when an electron transits across a surface. Consequently a carrier injected in dye-sensitization could traverse some distance ballistically[4] or tunnel across thin layers of insulators or semiconductors.[5−17] It has been shown that photoexcitation of dye molecules anchored to ultrathin (≤1 nm) outer shells of insulators or semiconductors on n-type semiconductor crystallites results electron transfer to the inner core material.[5−17] A recent report indicates that the electrons released in photoexcitation of dye molecules coated on a 10−50 nm gold film, move ballistically across and enter the CB of a n-type semiconductor.[18] The above effects have the potential of utilization in solar cells and optoelectronic devices. Here we show that the ability of dye-sensitization to release energetic electrons or holes could be exploited to construct photovoltaic cells incorporating several pigments, thereby broadening the spectral response with an enhancement of the efficiency.

To demonstrate the above ideas we fabricated photovoltaic cells of following heterostructure configurations. (i) **Configuration [1]** n-TiO_2/D_1/p-CuSCN: Nanocrystalline film of n-TiO_2 coated with a monolayer of dye D_1 followed by a thick outer layer of p-CuSCN. (ii) **Configuration [2]** n-TiO_2/*p-CuSCN*/D_2/p-CuSCN: Nanocrystalline film of n-TiO_2 covered with an ultrathin layer of *p-CuSCN*, a monolayer layer of dye D_2 on *p-CuSCN* surface, and finally a thick outer layer of p-CuSCN. (The thin inner layer is indicated in italics to distinguish from the thick layer.) (iii) **Configuration [3]** TiO_2/D_1/*p-CuSCN*/D_2/p-CuSCN: Nanocrystalline film of TiO_2 coated with the dye D_1, a thin layer of *p-CuSCN* above D_1, a layer of dye D_2 on the *p-CuSCN* surface, and finally a thick layer of p-CuSCN.

TiO_2 films were deposited on conducting tin oxide (CTO) glass plates by the method described previously.[19] Films prepared by this method have a thickness of 8−10 μm and roughness factors of the order 300−400. Films of CuSCN (p-type semiconductor of band gap 3.6 eV[20]) were deposited from a solution in propyl sulfide by the method reported earlier[21]. The thicknesses of *p-CuSCN* layers were estimated as $t = W/AR\rho$ (W = wt. of CuSCN in the solution used for coating the film, A = film area, R = roughness factor of the film, and ρ = density of CuSCN). We have selected Fast Green (FG) and Acridine Yellow (AY) thiocyanate as the dyes D_1 and D_2 for the following reasons. The anionic dye FG strongly surface chelates to TiO_2, absorbs in the red region of the spectrum (peak at ∼ 650 nm), and has ground ($S°_1$) and excited ($S*_1$) levels permitting electron injection to the CB of TiO_2 and hole injection to VB of CuSCN. Furthermore, FG adsorbed on TiO_2 does not dissolve into the propyl sulfide solution during the coating process. The thiocyanate of the cationic dye AY readily anchors to the CuSCN surface, absorbs in the blue region (absorption peak at ∼ 470 nm), and its ground ($S°_2$) and excited ($S*_2$) levels allow electron and hole injection to TiO_2 and CuSCN, respectively. Again AY adsorbed on the CuSCN surface is not dissolved by propyl sulfide, enabling deposition of an over layer of CuSCN. The dye coverage in all configurations corresponded approximately to a monolayer. To construct the photovoltaic cell, the final layer of CuSCN was build up just above the topmost level of TiO_2 by repeated spreading of the coating solution and sintering. The outer CuSCN surface was painted with graphite to improve the ohmic contact, and a gold plated CTO glass plate pressed onto this surface served as the back contact (Figure 1). $I-V$ characteristics of the cells were recorded

* Corresponding author. E-mail: tenna@ifs.ac.lk.

10.1021/jp0348979 CCC: $25.00
Published on Web 11/22/2003

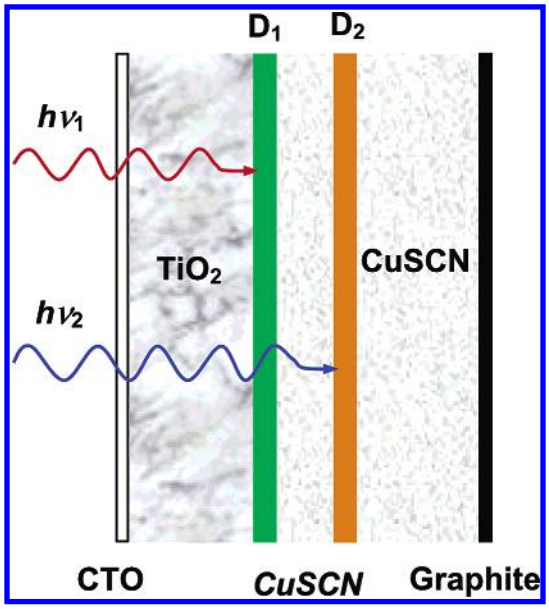

Figure 1. Diagram illustrating the construction of the photovoltaic cell of heterostructure configuration $TiO_2/D_1/p\text{-}CuSCN/D_2/p\text{-}CuSCN$. The green region indicates the dye D_1 (Fast Green) anchored to TiO_2 and orange region the dye D2 (Acridine Yellow) anchored to the outer surface of the thin (~2 nm) layer of *p-CuSCN*. The thick layer of p-CuSCN is deposited on top of the dye D_2. Current leads are connected to graphite and conducting tin oxide (CTO) surfaces.

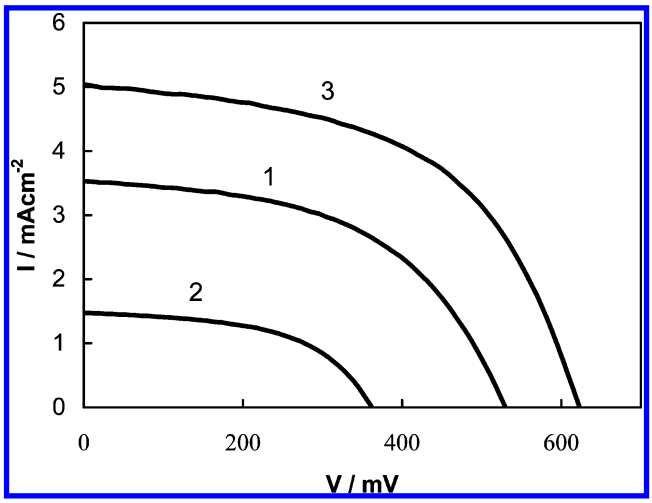

Figure 2. *I*−*V* characteristics of the cells [1] $TiO_2/D_1/p\text{-}CuSCN$, [2] $TiO_2/p\text{-}CuSCN/D_2/p\text{-}CuSCN$, and [3] $TiO_2/D_1/p\text{-}CuSCN/D_2/p\text{-}CuSCN$. D_1 = Fast Green, D_2 = Acridine Yellow.

at 1000 Wm^{-2} using a xenon lamp as the light source without a UV filter. Table 1 gives short-circuit photocurrent (I_{sc}), open-circuit voltage (V_{oc}), and fill factor (FF) of the cells of different heterostructure configurations. Samples of same characteristics (i.e., TiO_2 film thickness ~8 μm, calculated *p-CuSCN* film thickness 2 nm, and p-CuSCN film thickness ~10 μm) are selected for comparison. We could not confirm whether *p-CuSCN* layers have uniform thickness.

However, results reported on the basis of the average film thickness (computed from the amount CuSCN used) gave reproducible results. When a UV filter was used, I_{sc} and η dropped by about 8−10% with an insignificant change in V_{oc}. It is interesting to note that the drop in I_{sc} after insertion of the UV filter is not very significant. UV irradiation increases the conductivity of CuSCN (UV generates band-gap carriers and/or liberates SCN which acts as a dopant). Although a large contribution to I_{sc} would be expected by UV-generated carriers

TABLE 1: Short-Circuit Photocurrent (I_{sc}), Open-Circuit Voltage (V_{oc}), Fill Factor (FF), and Efficiency (η) of Photovoltaic Cells of Different Configurations

cell configuration	I_{sc} (mA/cm^2)	V_{oc} (mV)	FF%	η%
$TiO_2/D_1/p\text{-}CuSCN$	3.5	528	51.3	0.95
$TiO_2/D_2/p\text{-}CuSCN$	0.6	356	50.0	0.10
$TiO_2/p\text{-}CuSCN/D_2/p\text{-}CuSCN$	1.4	370	51.7	0.28
$TO_2/D_1/p\text{-}CuSCNS/D_2/p\text{-}CuSCNS$	5.0	634	52.5	1.67

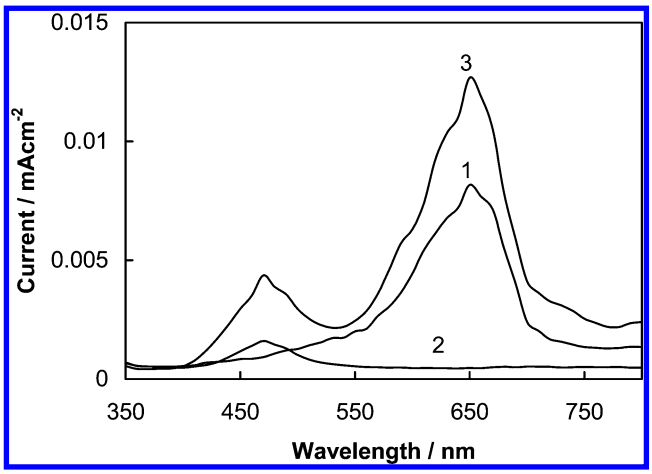

Figure 3. Photocurrent action spectra of the cells [1] $TiO_2/D_1/p\text{-}CuSCN$, [2] $TiO_2/p\text{-}CuSCN/D_2/p\text{-}CuSCN$, and [3] $TiO_2/D_1/p\text{-}CuSCN/D_2/p\text{-}CuCNS$.

TABLE 2: Incident Photon to Photocurrent Conversion Efficiencies (IPCEs) of Cells of Different Configurations at the Peak Absorption Wavelengths of the Two Dyes D_1 (FG, 650 nm) and D_2 (AY, 470 nm)

cell configuration	IPCE (D_1, λ_{peak}= 650)	IPCE (D_2, λ_{peak}= 470)
$TiO_2/D_1/p\text{-}CuSCN$	15.6%	
$TiO_2/p\text{-}CuSCN/D_2/p\text{-}CuSCN$		6.9%
$TiO_2/D_1/p\text{-}CuSCN/D_2/p\text{-}CuSCN$	36.2%	28.2%

in TiO_2 and/or CuSCN, the increase in conductivity promotes recombination of visible light-generated charges across the *p-CuSCN* barrier. Thus, the expected increase in I_{sc} by UV is largely compensated by a recombination loss.

I−*V* characteristics of the cells (Figure 2) and data presented in Table 1 show that the double-dye system of configuration [3] yields the highest values for all the above parameters with an efficiency of 1.67% compared to 0.95% and 0.28% respectively for the single dye systems of configurations [1] and [2].

The photocurrent action spectra of the cells of different configurations presented in Figure 3 clearly show that in the double-dye system both D_1 and D_2 contribute to the photocurrent. It is surprising to note that the incident photons to photocurrent conversion efficiencies (IPCEs) at the absorption peaks of the two dyes are higher in the double dye system compared to configurations [1] and [2] with the individual dyes (Table 2).

The cell of configuration [1] is a standard dye-sensitized solid-state cell (DS SSC) where n- and p-type semiconductors sandwich a dye monolayer. Here the excited dye molecules inject electrons and holes to the n and p-type materials.

DS SSCs have low I_{sc} and V_{oc} values because of the rapid recombination of injected electrons and holes. Electrons (holes) in the n-type (p-type) material could move to the p-type (n-type) region by tunneling across the dye monolayer. Perhaps the trap states at the interface mediate the recombination. In a cell of configuration [2], p-CuSCN surfaces on either side

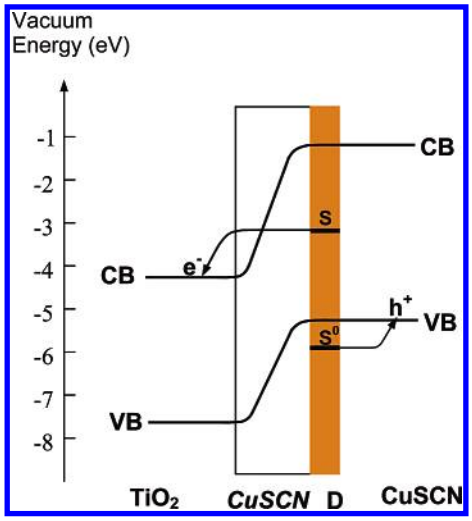

Figure 4. Energy level diagram showing the band structure in n-TiO_2/*p-CuSCN*/D/p-CuSCN, ground (S°) and excited (S*) levels of the dye D and the modes of electron−hole transfer when the dye is photoexcited. The electron tunnels through the thin (∼2 nm) layer of *p-CuSCN* and moves to the conduction band of TiO_2, releasing a hole to the thick layer of p-CuSCN.

interpose the dye monolayer. Existence of a photovoltaic effect of the same sign as in the configuration [1] shows that photoexcited dye molecules D^*_2 inject electrons and holes to n-TiO_2 and p-CuSCN, respectively, i.e.,

$$h\nu_2 + \text{n-TiO}_2/p\text{-}CuSCN/\text{D}_2/\text{p-CuSCN} \rightarrow \text{n-TiO}_2/p\text{-}CuSCN/\text{D}^*_2/\text{p-CuSCN} \rightarrow \text{n-TiO}_2(\text{e}^-)/p\text{-}CuSCN/\text{D}_2/\text{p-CuSCN}\,(\text{h}^+) \quad (1)$$

Therefore, we conclude that, on de-excitation of D^*_2 an electron is transferred to n-TiO_2 via tunneling across *p-CuSCN* and concomitantly releasing a hole to p-CuSCN. As expected, I_{sc} and V_{oc} of the cell decrease with the increase of the thickness of the *p-CuSCN* barrier. Experimentally, the optimum thickness was found to be 2−3 nm. Attempts to reduce the thickness further (i.e., by using more dilute solution of CuSCN for the deposition of films) seem to produce imperfect films populated with voids. When the thickness of *p-CuSCN* exceeds ∼15 nm, the photovoltaic effect in configuration [2] becomes undetectable. In this situation D^*_2 is created in a nearly symmetric environment and sees no potential gradient favoring charge transfer. An energy level diagram illustrating the electron and hole transfers and the bending of the bands is presented in Figure 4.

Charge separation in a cell of configuration [3] involves tunneling of both electrons and holes through a barrier of *p-CuSCN*. Here on excitation, D_1 an electron transfers to n-TiO_2 and the hole generated tunnels through the barrier *p-CuSCN*/D_2 in reaching the p-CuSCN anode. We summarize electron−hole separation originating from excitation of D_1 as

$$h\nu_1 + \text{n-TiO}_2/\text{D}_1/p\text{-}CuSCN/\text{D}_2/\text{p-CuSCN} \rightarrow \text{n-TiO}_2/\text{D}^*_1/p\text{-}CuSCN/\text{D}_2/\text{p-CuSCN} \rightarrow \text{n-TiO}_2\,(\text{e}^-)/\text{D}_1/p\text{-}CuSCN/\text{D}_2/\text{p-CuSCN}\,(\text{h}^+) \quad (2)$$

Similarly on excitation of D_2, a hole moves to p-CuSCN and an electron tunnels to n-TiO_2 through the barrier D_1/*p-CuSCN*. We summarize the resulting charge separation as

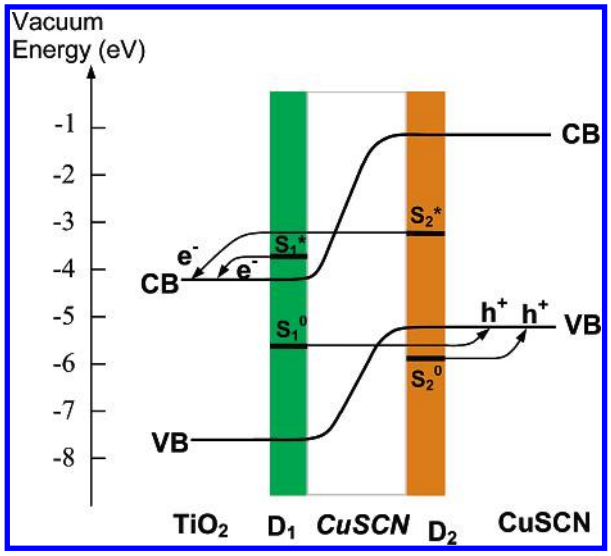

Figure 5. Energy level diagram showing the band structure in TiO_2/D_1/*p-CuSCN*/D_2/p-CuSCN, the positions of the ground ($S°_1$,$S°_2$) and excited (S^*_1,S^*_2) levels of the two dyes (D_1,D_2). The dyes D_1 (FG) and D_2 (AY) are anchored to TiO_2 and *p-CuSCN*, respectively.

$$h\nu_2 + \text{n-TiO}_2/\text{D}_1/p\text{-}CuSCN/\text{D}_2/\text{p-CuSCN} \rightarrow \text{n-TiO}_2/\text{D}_1/p\text{-}CuSCN\,/\text{D}^*_2/\text{p-CuSCN} \rightarrow \text{n-TiO}\,(\text{e}^-)/\text{D}_1/p\text{-}CuSCN/\text{D}_2/\text{p-CuSCN}\,(\text{h}^+) \quad (3)$$

Location of the excited states S^*_1 and S^*_2 of the two dyes above the CB of n-TiO_2 and ground levels $S°_1$ and $S°_2$ below the VB position of CuSCN (Figure 5) permit the above charge transfers energetically.

Band bending in the region of the heterostructure interface, facilitating charge transfer, is also indicated in Figure 5. Band bending could begin at the dye monolayers; for clarity we have not depicted this in Figure 5. In a cell of configuration [1], the monolayer of the dye D_1 is the barrier separating the relaxed electron−hole pair. However, in configuration [3], a wider barrier D_1/*p-CuSCN*/D_2 separates the electrons and holes relaxed to the CB and VB of n-TiO_2 and p-CuSCN, respectively. The energy of the geminate electron−hole pair enables achieving wide charge separation after tunneling through the barriers. After relaxation to the band edge energies, reverse tunneling leading to recombination is greatly reduced, because the tunneling probability depends on particle energy. As recombination is better suppressed, IPCEs corresponding to peak absorption positions of both the dyes D_1 and D_2 reach strikingly higher values in configuration [3] compared to the configurations based on individual dyes. Although thicker barriers are more effective in mitigating recombination, they also reduce the injection rate. Thus the barrier width needs to be tuned to an optimum to achieve the maximum IPCE. We believe that for similar reasons the double-dye cell attains a higher V_{oc}. The difference in quasi-Fermi levels (QFL) of electrons in the p- and n-type regions measures the V_{oc}, and the gap between the VB and CB edges determines an upper limit to this quantity. When the barriers suppress recombination, buildup of QFLs enhances the V_{oc}.

We have also constructed several other semiconductor/dye heterostructures with a view of understanding the charge transfer and recombination mechanisms. A cell of configuration [1] with D_1 replaced by D_2 gave I_{sc} and V_{oc} much less than that of the configuration [2] with the same dye. (Table 1). Here again the reason seems to be suppression of recombination by the *p-CuSCN* barrier in the former system. Cells where two dyes are deposited one on top of the other (i.e., heterostructures of

the form n-TiO_2/D_1D_2/p-CuSCN) are not expected to perform satisfactorily owing to mutual deactivation of D^*_1 and D^*_2 in close proximity (concentration quenching). With dyes D_1 (= FG) and D_2 (= AY), the above heterostructure could not be satisfactorily constructed as D_2 is not adsorbed on D_1-coated TiO_2. When D_2 was painted over D_1 the cell out-put was found to be very much inferior to that of configuration [3]. The possibility exists that suitable combination of other dyes may overcome concentration quenching if the rates of charge transfer, energy transfer, or injection competes favorably with concentration quenching.

The above technique can be extended to form heterostructures constituted of more than two dyes. The photocurrent action spectrum of a model three-dye system, which we have constructed, i.e., n-TiO_2/D_1/*p-CuSCN*/D_2/*p-CuSCN*/D_3/p-CuSCN (D_1 = FG, D_2 = AY, D_3 = Rhodamine 6G), displayed contributions of all three components. Unfortunately we did not succeed in improving the efficiency above the two-dye system. Thicker barriers in this case reduce electron and hole tunneling probabilities. Our fabrication technique at this stage does not permit deposition of *p-CuSCN* layers of thickness <2 nm. The open-circuit voltage and the efficiency we obtained for the double dye system is significant for a DS SSC[19,21−29] that utilizes readily available organic sensitizers. Further improvements would depend on identification of dyes with appropriate energy level positions and optical absorption characteristics and on developing methods for depositing ultrathin layers of high band gap semiconductors on nanostructured surfaces. Ordering of the dye layers to take advantage of wavelength-dependent light scattering in the nanocrystalline matrix would also be important.

Experimental Details. Nanocrystalline TiO_2 films of the type suitable for construction of dye-sensitized solid-state solar cells were deposited on CTO glass plates (15 ohm sq^{-1}, plate area = 1.5 × 0.5 cm^2, film area = 0.25 cm^2) by the method described in ref 19. Briefly, the procedure involved painting of a colloidal solution of TiO_2 (prepared by hydrolysis of titanium isopropoxide) on CTO glass surface heated to ∼150 °C and sintering at 450 °C for 10 min. After rubbing off the loose crust with cotton wool, the process is repeated until a film of ∼8−10 μm is formed. The average film thickness was determined using a profile meter, which scanned the film surface. CuSCN was deposited by evenly spreading a measured amount of solution of CuSCN in propyl sulfide (40 mg in 10 mL) on sample plates heated to ∼90 °C and sintering at same temperature for a few minutes. The films were then dried in a warm air current to expel excess propyl sulfide.

Commercially available dyes, Fast Green, Rhodamine 6G, and Acridine Yellow (Aldrich), were used without further purification. Chloride forms of Rhodamine 6G and Acridine Yellow were converted into their respective thiocyanates as follows. The solid dye in the chloride form was boiled with an excess saturated aqueous solution of KSCN (for ∼30 min), where the thiocyanated dye is insoluble. The solid was separated by centrifugation and rinsed with water. The procedure was repeated to complete the double decomposition reaction, which precipitated the less soluble thiocyanate of the dye. Thiocynated dyes were further purified by recrystallization from alcoholic solution. Fast Green was deposited on TiO_2 films by keeping the plate immersed in an alcoholic solution of the dye (1.0×10^{-3} M), rinsing with alcohol, and drying. Acridine Yellow was deposited by exposing the CuSCN surface to a solution of Acridine Yellow thiocyanate in alcohol (0.8×10^{-3} M) for 15−20 min. The amounts of dyes adsorbed on different surfaces were estimated by noticing the depletion of dye in coating solutions spectrophotometrically.

A gold-plated CTO glass surface pressed onto the graphite surface served as the back contact. $I-V$ characteristics were obtained using a source meter (Keithley), and the intensity of the 500 W xenon lamp used was measured with a Pyranometer (Eko). Intensity of the monochromator output was recorded using a calibrated silicon detector.

References and Notes

(1) Miller, R. J. D.; McLendon, G. L.; Nozik, A. J.; Schmickler, W.; Willig, F. *Surface Electron-Transfer Processes*; VCH: Weinheim 1994; pp 167−302.

(2) Hagfeldt, A.; Gratzel, M. *Chem. Rev.* **1995**, *95*, 49.

(3) Asbury, J. B.; Hao, E.; Wang, Y.; Gosh, H. N.; Lain, T. *J. Phys. Chem. B* **2001**, *105*, 4545.

(4) Tennakone, K.; Kottegoda, I. R. M.; De Silva, L. A. A.; Perera, V. P. S. *Semicond. Sci. Technol*. **1999**, *14*, 975.

(5) Tennakone, K.; Bandaranayake, P. K. M.; Jayaweera, P. V. V.; Konno, A.; Kumara, G. R. R. A. *Physica E* **2002**, *14*, 190.

(6) Tennakone, K.; Bandara, J.; Bandaranayake, P. K. M.; Kumara, G. R. A.; Konno, A. *Jpn. J. Appl. Phys*. **2001**, *40*, L732.

(7) Kumara, G. R. R. A.; Tennakone, K.; Perera, V. P. S.; Konno, A.; Kaneko, S.; Okuya, M. *J. Phys. D: Appl. Phys*. **2001**, *34*, 868.

(8) Tennakone, K.; Perera, V. P. S.; Kottegoda, I. R. M.; De Silva, L. L. A.; Kumara, G. R. R. A.; Konno, A. *J. Electron. Mater*. **2001**, *30*, 992.

(9) Diamant, Y.; Chen, S. G.; Melamed, O.; Zaban, A. *J. Phys. Chem. B* **2003**, *107*, 1977.

(10) Chappel, S.; Chen, S. G.; Zaban, A. *Langmuir* **2002**, *18*, 3336.

(11) Chen, S. G.; Chappel, S.; Diamant, Y.; Zaban, A. *Chem. Mater*. **2001**, *13*, 4629.

(12) Chappel, S.; Chen, S. G.; Zaban, A. *Langmuir* **2002**, *18*, 3336.

(13) Palomares, E.; Clifford, J. N.; Haque, S. A.; Lutz, T.; Durrant, J. R. *J. Am. Chem. Soc*. **2003**, *125*, 475.

(14) Palomares, E.; Clifford, J. N.; Haque, S. A.; Lutz, T.; Durrant, J. R. *Chem. Commun*. **2002**, 1464.

(15) Kay, A.; Gratzel, M. *Chem. Mater*. **2002**, *14*, 2930.

(16) Bedja, I.; Kamat, P.V. *J. Phys. Chem*. **1995**, *99*, 9182.

(17) Tennakone, K.; Kumara, G. R. R. A.; Kottegoda, I. R. M.; Perera, V. P. S. *Chem. Commun*. **1999**, 15.

(18) McFarland, E. W.; Tang, J. *Nature* **2003**, *421*, 616.

(19) Tennakone, K.; Kumara, G. R. R. A.; Kumarasinghe, A. R.; Wijayantha, K. G. U.; Sirimanne, P. M. *Semicond. Sci. Technol*. **1995**, *10*, 1689.

(20) Tennakone, K.; Jayatiisa, A. H.; Fernando, C. A. N.; Wickramanayake, S.; Punchihewa, S.; Weerasena, L. K.; Premasiri, W. D. R. *Phys. Status Solidi A*, **1987**, *103*, 491.

(21) Kumara, G. R. R. A.; Konno, A.; Senadeera, G. K. R.; Jayaweera, P. V. V.; De Silva, D. B. R. A.; Tennakone, K. *Sol. Energy Mater. Sol. Cells* **2001**, *69*, 195.

(22) O'Regan, B.; Schwartz, D. T. *Chem. Mater*. **1995**, *7*, 1349.

(23) Tennakone, K.; Kumara, G. R. R. A.; Kottegoda, I. R. M.; Wijayantha, K. G. U.; Perera, V. P. S. *J. Phys. D: Appl. Phys*. **1998**, *31*, 1492.

(24) O'Regan, B.; Schwartz, *J. Appl. Phys*. **1996**, *68*, 2439.

(25) Bach, U.; Lupo, D.; Compte, P.; Moser, J. E.; Weissortel, F.; Salbeck, J.; Spreitzer, H.; Gratzel, M. *Nature* **1998**, *359*, 583.

(26) Kumara, G. R. A.; Konno, A.; Shiratsuchi, K.; Tsukahara, J.; Tennakone, K. *Chem. Mater*. **2002**, *14*, 954.

(27) O'Regan, B.; Schwartz, D. T.; Zakeeruddin, S. M.; Gratzel, M. *Adv. Mater*. **2000**, *12*, 1263.

(28) O'Regan, B.; Lenzmann, F.; Muis, R.; Wienke, J. *Chem. Mater*. **2002**, *14*, 5023.

(29) Meng, Q. B.; Zhang, X. T.; Sutano, I.; Rao, T. N.; Fujishima, A.; Takahashi, K.; Sato, O.; Watanabe, H.; Nakamori, T.; Uragami, M. *Proceedings of the 14th Intenational Conference on Photochemical Conversion of Solar Energy*, Sapporo, Japan, 2002, pp. W1−P− 62.